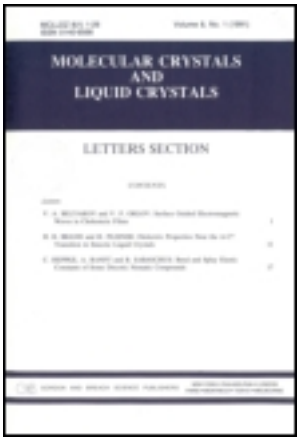

Molecular Crystals and Liquid Crystals
Publication details, including instructions for authors and subscription information:
http://www.tandfonline.com/loi/gmcl20

Synthesis of Reduced Graphene Oxide/Polypyrrole Conductive Composites

Niranjanmurthi Lingappan [a], Yeong-Soon Gal [b] & Kwon Taek Lim [a]
[a] Department of Imaging System Science, Pukyong National University, Busan, 608-737, Korea
[b] Polymer Chemistry Laboratory, College of Engineering, Kyungil University, Gyeongsan, 712-701, Gyeongsangbuk-Do, Republic of Korea
Published online: 08 Jan 2014.

To cite this article: Niranjanmurthi Lingappan, Yeong-Soon Gal & Kwon Taek Lim (2013) Synthesis of Reduced Graphene Oxide/Polypyrrole Conductive Composites, Molecular Crystals and Liquid Crystals, 585:1, 60-66, DOI: 10.1080/15421406.2013.849510

To link to this article: http://dx.doi.org/10.1080/15421406.2013.849510

Mol. Cryst. Liq. Cryst., Vol. 585: pp. 60–66, 2013

ISSN: 1542-1406 print/1563-5287 online
DOI: 10.1080/15421406.2013.849510

Taylor & Francis
Taylor & Francis Group

Synthesis of Reduced Graphene Oxide/Polypyrrole Conductive Composites

NIRANJANMURTHI LINGAPPAN,[1] YEONG-SOON GAL,[2] AND KWON TAEK LIM[1,*]

[1]Department of Imaging System Science, Pukyong National University, Busan 608-737, Korea
[2]Polymer Chemistry Laboratory, College of Engineering, Kyungil University, Gyeongsan 712-701, Gyeongsangbuk-Do, Republic of Korea

Reduced graphene oxide/polypyrrole (RGO/PPy) conductive composites were prepared by in-situ oxidative polymerization of pyrrole monomer in the presence of RGO under acidic condition. RGO used for the polymerization was previously prepared from natural graphite using modified Hummer's method, subsequently reduced using hydrazine hydrate. The structural, morphology and electrical property of the composites together with graphene oxide (GO) and RGO were characterized using FTIR, XPS, TGA, HRTEM and XRD. It was observed that the RGO and PPy formed a uniform composite with the PPy layers wrapped on the RGO surface. XRD results showed that the RGO/PPy composite was amorphous as neat PPy, suggesting the backbone structure of the PPy was not damaged by the introduction of RGO. Furthermore, the thermal and electrical properties of the composites were much higher than that of pure PPy thank of RGO.

Keywords Electrical conductivity; oxidative polymerization; polypyrrole; reduced graphene oxide

Introduction

Graphene, a new class of two-dimensional carbon nanostructure, owing to their excellent electronic transport properties, extremely high mechanical stiffness, large surface area, and exceptional thermal and electrical conductivity, has been predicted to hold great promise for many potential applications such as nanoelectronics, sensors, solar cells, and energy storage devices [1–5]. In particular, graphene can be a good candidate as nanofiller to enhance the mechanical and functional properties, including the electrical and thermal conductivities, of polymer-based composites [6–8]. Thus, many studies have been directed toward developing techniques to prepare graphene sheets.

On the other hand, supercapacitors have attracted a great deal of attention due to their high power density, long cycle life, and rapid charging/discharging rates. Based on the charge storage mechanism, they can be divided into two categories, namely electric

*Address correspondence to Prof. Kwon Taek Lim, Department of Imaging System Science, Pukyong National University, Busan 608-737, Korea (ROK). Tel.: (+82)51-629-6409; Fax: (+82)51-629-6408. E-mail: ktlim@pknu.ac.kr

double layer capacitors (EDLC) and pseudocapacitors. For EDLC, carbon-based materials with high surface area are usually used, while pseudocapacitors use conducting polymers (CPs) and metal oxides as electrode materials [9–10]. Among various CPs, polypyrrole (PPy) has been recognized as ideal electrode materials for pseudocapacitors. However, commercial application of PPy is restricted due to its low thermal stability and poor electrical conductivity [11]. It was also reported that the thermal stability and electrical properties of CPs could be greatly improved by the incorporation of graphene nanosheets [12–16]. The graphene intercalated composites have been prepared by various methods such as layer-by-layer assembly, solution mixing, electrostatic interaction. etc.

Towards this goal, reduced graphene oxide/polypyrrole (RGO/PPy) composites have been synthesized via in-situ oxidative polymerization using anhydrous $FeCl_3$ as an oxidant. The structure, morphology, thermal and electrical properties of the resulting hybrids were characterized and discussed in detail.

Experimental

Synthesis

Graphite powder, Pyrrole, anhydrous $FeCl_3$ and sodium borohydride ($NaBH_4$) were obtained from Sigma-Aldrich (Korea). Pyrrole monomer was distilled twice under reduced pressure before use. All other reagents (AR grade) were purchased from Junsei chemicals (Japan) and used as received without further purification.

Preparation of RGO

Graphite oxide was synthesized from graphite powder according to our previously reported method [17]. Briefly, 0.5 g of graphite powder, 2.5 g of $NaNO_3$ and 200 mL conc. H_2SO_4 were mixed in an ice-bath. Then, 15 g of $KMnO_4$ was added gradually with stirring, and the temperature of the mixture was not allowed to exceed 20 °C. The mixture was then stirred at 35 °C for 30 min. At the end of 30 min, 200 mL of de-ionized water was slowly added to the mixture, followed by stirring the mixture at 90 °C for 30 min. The reaction was terminated by addition of 500 mL of water and 10 mL 30% of H_2O_2 with stirring at 10 °C. The product was filtered and thoroughly washed with 5% HCl followed distilled water and dried under a vacuum at 50 °C for 24 h. The chemical reduction of the GO was carried out as follows. In brief, 0.5 g of GO was dispersed in 100 mL of water and ultrasonicated for 1 h. Then, 5 mL of hydrazine monohydrate was added and the solution heated in an oil bath at 100 °C for 24 h. The reduced GO was gradually precipitated out as a black solid. This product was isolated by filtration and washing copiously with water. The obtained RGO was dried under vacuum at 50 °C for 24 h.

In-situ synthesis of RGO/PPy composites

The RGO/PPy composite was synthesized via in-situ oxidative polymerization. In a typical method, 0.1 g of RGO and 2 g of anhydrous $FeCl_3$ were dispersed in 50 mL of distilled water with ultrasonication for 30 min. Then, 0.5 g of freshly distilled pyrrole monomer was added dropwise into the above dispersion and the reaction mixture was stirred at room temperature for 24 h. Finally, the reaction mixture was filtrated and rinsed with acetone and water repeatedly, and then dried under a vacuum at 40 °C for 24 h.

Characterization

Fourier transform infrared (FTIR) spectroscopic analysis was conducted on a Perkin-Elmer spectrometer in the range 4000–400 cm^{-1}. The samples were pressed into pellets with KBr powder. X-ray photoelectron spectroscopy (XPS) measurements were carried out on a Kratos AXIS Ultra HSA spectrometer equipped with a monochromatized Al Ka X-ray source (1468.6 eV photons). Thermal gravimetric analysis (TGA) was performed on a Perkin-Elmer Pyris 1 TGA at a heating rate of 10 °C min^{-1} under nitrogen atmosphere. High resolution transmission electron microscope (HRTEM) images were taken on a Hitachi, J-2100 (Japan) microscope. Powder X-ray diffraction (XRD) patterns were obtained by using a Rigaku diffractometer equipped with Cu Kα radiation ($\lambda = 0.15418$ nm). The room temperature electrical conductivity of the samples was measured by a standard four-probe method using a Keithley 2000 (USA) apparatus.

Results and Discussion

The FTIR spectra of GO, RGO, RGO/PPy composites and neat PPy, are presented in Fig. 1. The FTIR spectrum of GO shows a broad absorption at 3370 cm^{-1} is ascribed to the O—H stretching vibration. The strong peak at 1730 cm^{-1} is assigned to the C=O stretching vibration of the carboxylic acid and carbonyl moieties. Besides, it also shows some bands due to C—O (1400 cm^{-1}), epoxy C—O (1220 cm^{-1}) and alkoxy C—O (1050 cm^{-1}) groups situated at the edges of the GO sheets. In the case of RGO, the sharp band at 1560 cm^{-1}, corresponds to the skeletal vibration of graphene nanostructure. As can be clearly seen (Fig. 1(c)), the RGO/PPy and neat PPy (Fig. 1(d)) display very similar spectra. In the case of PPy, the bands at 1585 and 1480 cm^{-1} are correspond to the PPy ring vibrations. The bands at 1340 and 1030 cm^{-1} are associated with the C—H band in-plane vibration and N—H in-plane deformation, respectively. Additionally, the peak at 1150 cm^{-1} is ascribed to the N—C stretching band, while the peak observed at 920 cm^{-1} corresponds to the C—H

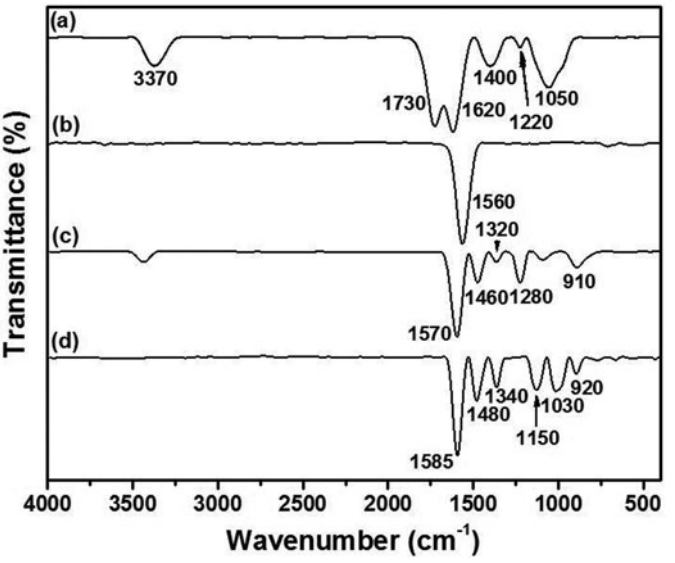

Figure 1. FTIR spectra of (a) GO, (b) RGO, (c) RGO/PPy composites and (d) neat PPy.

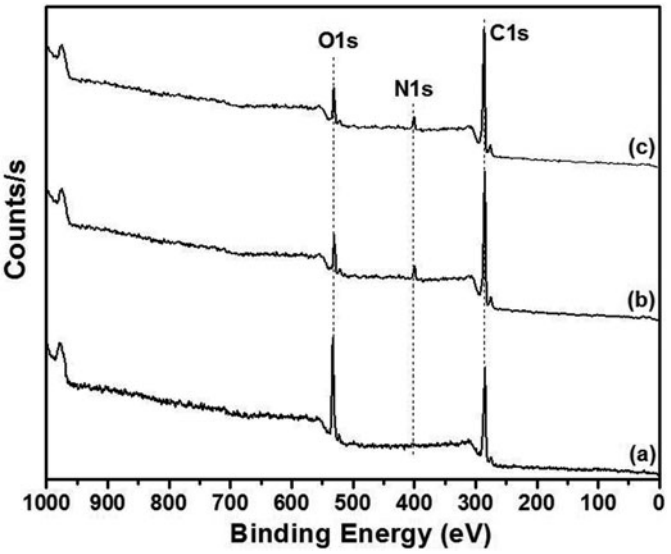

Figure 2. XPS spectra of (a) GO, (b) RGO and (c) RGO/PPy composites.

out-of-plane vibration indicating the polymerization of pyrrole [18]. It can be observed that all the above characteristic peaks of PPy are clearly observed in the spectrum of the RGO/PPy nanocomposites. However, the peak corresponding to the RGO is almost disappeared, indicating the thin PPy layers were well coated on the surfaces of the RGO. Furthermore, the stretching vibration of PPy backbone at 1480 cm^{-1} is shifted to 1460 cm^{-1} which further confirms the noncovalent interaction between the graphitic structure and PPy ring [19].

The XPS spectra of pristine graphite, GO and RGO/PPy composites are shown in Fig. 2. The spectrum of GO dispalys two major component at 285.5 and 533.5 eV, correspond to the carbon and oxygen atoms, respectively. Compared to the GO, the signal at 533.5 eV is reduced significantly in the RGO, indicating the presence of removal of some oxygen-containing groups due to the chemical reduction. However, after in-situ polymerization, the RGO/PPy composite reveals a new peak at 399 eV is attributed to the nitrogen atoms. This result clearly suggested the presence of the PPy structure in the composites.

Figure 3 displays the TGA curves of pristine graphite, GO, RGO, RGO/PPy composites and neat PPy under nitrogen atmosphere. Pristine graphite is highly stable and there is no mass loss until 700 °C, while the GO exhibits a weight loss below 250 °C, corresponds to the thermal decomposition of oxygen-containing groups on the surfaces of GO. The TGA of the RGO displays only 10% weight loss, indicates its thermal stability. In the case of pristine PPy, two step decomposition profile is observed, the initial weight loss around 150 °C due to the evaporation of water and the main weight loss around 350 °C to 450 °C due to main-chain pyrolysis. The TGA curve of the RGO/PPy composites also shows the similar decomposition profile as that of neat PPy. The major weight loss between 280 and 450 °C, associated with the decomposition of PPy layer on the surfaces of RGO. However, in comparison to neat PPy, RGO/PPy composite shows the improved thermal stability due to the intrinsic properties of the RGO.

The morphology of the neat RGO and its composites are investigated using HRTEM. The HRTEM images of RGO and GO/PPy composites are shown in Fig. 4. The TEM

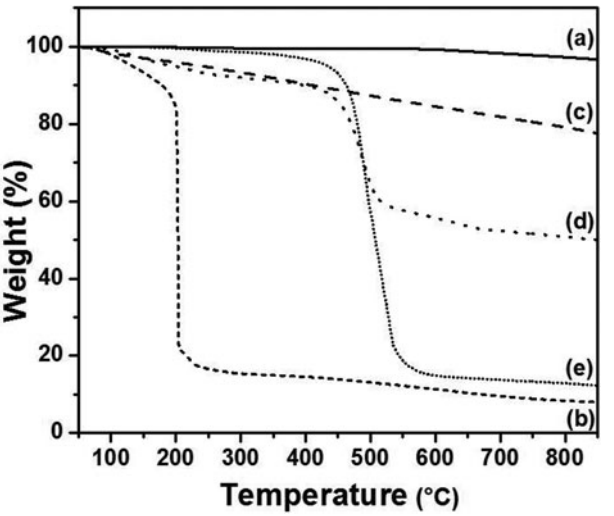

Figure 3. TGA curves of the (a) pristine graphite (b) GO, (c) RGO, (d) RGO/PPy composites and (e) neat PPy.

specimens are prepared by dipping the solution on a copper grid and dried in air. As can be seen Fig. 4, the HRTEM image of RGO/PPy shows quite different morphology from that of RGO. HRTEM image of the RGO shows a transparent lamellar structure. After in-situ polymerization, the surface of the RGO is masked by the dark PPy layers, which is attributed the strong interaction between the two components.

The XRD patterns of pristine graphite, GO, RGO, RGO/PPy composites and neat PPy are shown in Fig. 5. The pristine graphite shows a very strong peak at 26.4 ° and while the GO exhibits a broad peak at 10.45 °, indicating a complete oxidation of pristine graphite. After reduction, the original GO peak is disappeared and a new broad band is observed at 26.3 ° corresponds to the graphitic nanostructure. The XRD pattern of the neat PPy shows a broad peak at about 20 °, suggesting an amorphous structure of the polymer. However, the RGO/PPy composite displays a low intense broad peak in the range from at 19.5 to

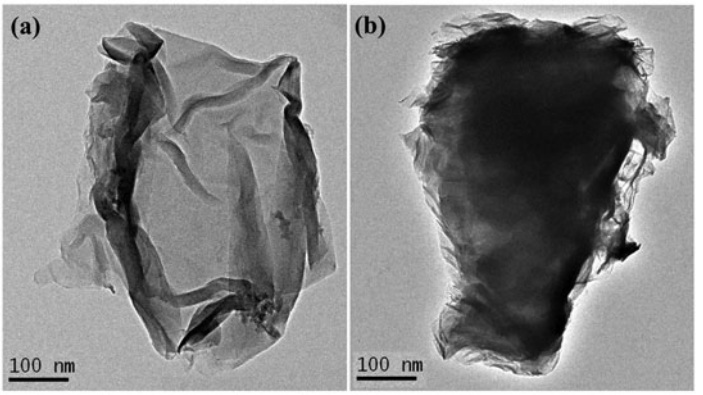

Figure 4. HRTEM images of the (a) RGO and (b) RGO/PPy composites.

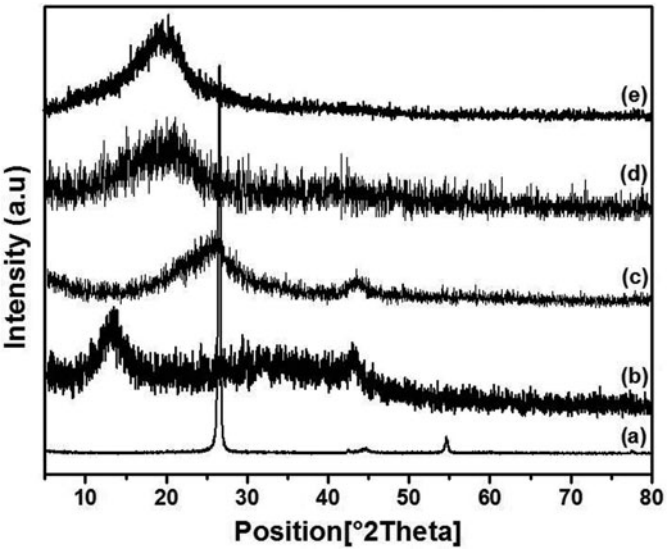

Figure 5. XRD patterns of the (a) pristine graphite (b) GO, (c) RGO, (d) RGO/PPy composites and (e) neat PPy.

23.5 °, corresponding to the PPy diffraction peak and the original diffraction peak of RGO is disappeared in the composites. The results clearly indicate that a thin layer is formed on the surface of RGO during the polymerization.

A standard four-point probe method is used to measure the conductivity of the composites. The room temperature electrical conductivity of the pure polymer and its composites is determined to be 0.21 and 1.6 S/cm, respectively. Thus, the RGO/PPy composite reveals an enhanced conductivity due to the conducting properties of the RGO.

Conclusions

We have synthesized RGO/PPy nanocomposites via in-situ oxidative polymerization. RGO was prepared from natural graphite using modified Hummer's, which served as a template for the polymerization. The structure and morphology of the fabricated composites were investigated by FTIR, XPS, TGA, HRTEM and XRD. The results revealed that the RGO/PPy composites were successfully prepared via π-π interaction between the RGO sheets and PPy chains. The electrical conductivity of the composites was calculated to be 1.6 S/cm. Furthermore, the thermal stability of the RGO/PPy composites improved significantly due to the intrinsic properties of the RGO.

Acknowledgment

This work was financially supported by the Joint Program of Cooperation in Science and Technology through NRF grant (Project no. 2011-0025680) of the Ministry of Education, Science and Technology (MEST) of Korea.

References

[1] Geim, A. K., & Novoselov, K. S. (2007). *Nat. Mater.*, *6*, 183.
[2] Allen, M. J., Tung, V. C., & Kaner, R. B. (2010). *Chem. Rev.*, *110*, 1321.
[3] Geim, A. K. (2009). *Science*, *324*, 1530.
[4] Kotov, N. A. (2006). *Nature*, *442*, 254.
[5] Li, Y., Fan, X. B., Qi, J. J., Ji, J. Y., Wang, S. L., Zhang, G. L., & Zhang, F. B. (2010). *Mater. Res. Bull.*, *45*, 1413.
[6] Stankovich, S., Dikin, D. A., Dommett, G. H. B., Kohlhaas, K. M., Zimney, E. J., & Stach, E. A. (2006). *Nature*, *442*, 282.
[7] Kim, J. S., Yun, J. H., Kim, I., & Shim, S. E. (2011). *J. Ind. Eng. Chem.*, *17*, 325.
[8] Otieno, G., & Kim, J. Y. (2008). *J. Ind. Eng. Chem.*, *14*, 187.
[9] Frackowick, E. (2009). *Phys. Chem. Che. Phys.*, *9*, 1774.
[10] Inagaki, M., Konna, H., & Tanaike, O. (2010). *J. Power Sources*, *195*, 7880.
[11] Park, J. H., Ko, J. M., Park, O. O., & Kim, D. W. (2002). *J. Power Sources*, *105*, 20.
[12] Matsuo, Y., Tahara, K., & Sugie, Y. (1997). *Carbon*, *35*, 113.
[13] Liu, P. G., Gong, K. C., Xiao, P., & Xiao, M. (2000). *J. Mater. Chem.*, *10*, 933.
[14] Cassagneau, T., & Fendler, J. H. (1998). *Adv. Mater.*, *10*, 877.
[15] Kovtyukhova, N. I., Ollivier, P. J., Martin, B. R., Mallouk, T. E., Chizhik, S. A., & Buzaneva, E. V. (1999). *Chem. Mater.*, *1*, 771.
[16] Wu, J. H., Tang, Q. W., Sun, H., Lin, J. M., Ao, H. Y., & Huang, M. L. (2008). *Langmuir*, *24*, 4800.
[17] Niranjanmurthi, L., Park, C., & Lim, K. T. (2012). *Mol. Cryst. Liq. Cryst.*, *564*, 206.
[18] Guo, H. F., Zhu, H., Lin, H. Y., & Zhang, J. Q. (2008). *Colloid. Polym. Sci.*, *286*, 587.
[19] Mandal, A., & Nandi, A. K. (2012). *J. Phys. Chem.*, *116*, 9360.